Int. J. Exp. Path. (1995), **76**, 381–390

Evolution of endotoxin induced acute lung injury in the rat

LOLA DOMENICI-LOMBARDO, CHIARA ADEMBRI*, MATTEO CONSALVO†, ROSSELLA FORZINI*, MONICA MEUCCI*, PAOLO ROMAGNOLI AND GIAN PAOLO NOVELLI*

*Department of Human Anatomy and Histology and *Institute of Anesthesiology and Intensive Care, University of Florence; †Department of Radiology, USL 10A Florence, Italy*

Received for publication 20 March 1995
Accepted for publication 20 July 1995

Summary. To clarify the evolution of acute lung injury induced by endotoxin, the progression of lung damage in 26 rats submitted to intratracheal instillation of 5 mg/kg body weight endotoxin was examined by blood gas analysis, computerized tomography, light and electron microscopy. Hypoxaemia, hypercapnia, acidosis and inhomogeneous bilateral infiltrates developed gradually within 48 hours. Monocytes appeared within blood capillaries and the instertitium by 12 hours after treatment, then migrated into alveoli and underwent progressive differentiation into macrophages by 24 hours after treatment. Granulocytes were found within blood capillaries at an early stage, but outside capillaries only at 48 hours. Hyperplasia of type II pneumocytes and hypertrophy of interstitial fibroblasts also occurred at 48 hours. These data suggest that the pathogenesis of endotoxin induced pulmonary injury proceeds through an early phase of granulocyte migration inside capillaries and monocyte extravasation, an intermediate phase of monocyte differentiation into macrophages inside alveoli and a late phase of diffuse infiltration of alveoli by newly differentiated macrophages and late-extravasated neutrophils.

Keywords: acute respiratory distress syndrome, ARDS, lipopolysaccharide, macrophages, neutrophils, septic shock

Endotoxin, a lipopolysaccharide (LPS) from the cell wall of Gram-negative bacteria, causes severe injury to the lung, as demonstrated in the sheep (Esbenshade *et al.* 1982; Meyrick & Brigham 1983) and rat (Simons *et al.* 1991; Adembri *et al.* 1992; Wheeldon *et al.* 1992). In humans, endotoxin is believed to be responsible for lung injury during septic shock, leading to the onset of acute 'adult respiratory distress syndrome' (ARDS) (Weiner-Kronish *et al.* 1990), a life-threatening disease. In the survivors, lung injury can heal or evolve into fibrosis (chronic ARDS) (Hasleton 1983; Murray *et al.* 1988).

Correspondence: Dr L. Domenici-Lombardo, Department of Human Anatomy and Histology, Section 'E. Allara', Viale Pieraccini 6, I-50139 Florence, Italy.

Inflammatory cell (neutrophil and macrophage) infiltration into the alveoli and septa is a key feature of acute ARDS (Bachofen & Weibel 1982), whereas neutrophil infiltration seems of primary importance in experimental, endotoxin induced lung injury (Simons *et al.* 1991; Tate & Repine 1983; Ooi *et al.* 1994).

Endotoxaemia is a major complication of severe trauma and intensive care treatment whatever the cause (Kaplan *et al.* 1979; Fein *et al.* 1983; Glauser *et al.* 1991); this explains the interest in understanding the pathogenesis of endotoxin induced lung injury, as a premise for effective prevention and treatment.

Since the cellular composition and the time-course of endotoxin induced lung infiltrates are still to be determined, we addressed these issues experimentally in the

rat, upon intratracheal instillation of a definite dose of LPS, which has been demonstrated to produce selective and progressive lung damage (Adembri *et al.* 1992).

Material and methods

Experiments were performed on male Wistar rats (mean weight 325 ± 30 g). Animals were fed *ad libitum* until 18 hours before the procedures and had free access to water.

The experiments were performed adhering to the guidelines of the Council for International Organizations of Medical Sciences and the Italian law for the use of experimental animals.

Rats were pretreated with atropine (0.01 mg/kg i.p.), anaesthetized with ketamine (60 mg/kg i.p.; Ketalar, Parke-Davis, Milan, Italy) and placed head-down on a table inclined at 45°.

After surgical exposition of the trachea, a thin needle was inserted into the trachea to instill the solutions to be tested.

The animals were divided into three groups:

sham operated, otherwise untreated ($n = 8$);
instilled with saline (0.9% NaCl), 0.125 ml ($n = 14$);
instilled with endotoxin (lipopolysaccharide B, serotype 0111: B4, Difco Laboratories, Detroit, Mi, USA), 5 mg/kg dissolved in 0.125 ml saline ($n = 26$).

For haematological, radiological and histological assays, rats were anaesthetized again as described above.

All the animals survived until the end-point, i.e. 12, 24 or 48 hours after treatment.

The following analyses were performed at baseline and at 12, 24 and 48 hours after instillation:

arterial gas analyses (Po_2, Pco_2, pH);
thoracic computerized tomography (CT);
light and electron microscopy.

Arterial gas analyses

Blood samples were taken from abdominal aorta of 24 rats. Arterial gas analyses were performed by a micromethod with an automatic instrument (IL1312, Milan, Italy).

Computed tomography (CT)

CT scans were performed by a CX/S tomoscan device (Philips, Eindhoven, Netherlands) on 2 untreated, 6 saline instilled and 10 endotoxin instilled rats.

The scans were obtained in continuous slices 2 mm in thickness with a matrix at high resolution (512 × 512 pixels, 120 kV, 120 mA, 2.8 s); scans were post-processed with reconstruction at high resolution by convolution filter no. 4.

Microscopy and morphometry

The lungs of each rat were divided into two halves with a section through the hilus, apex and basis. For light

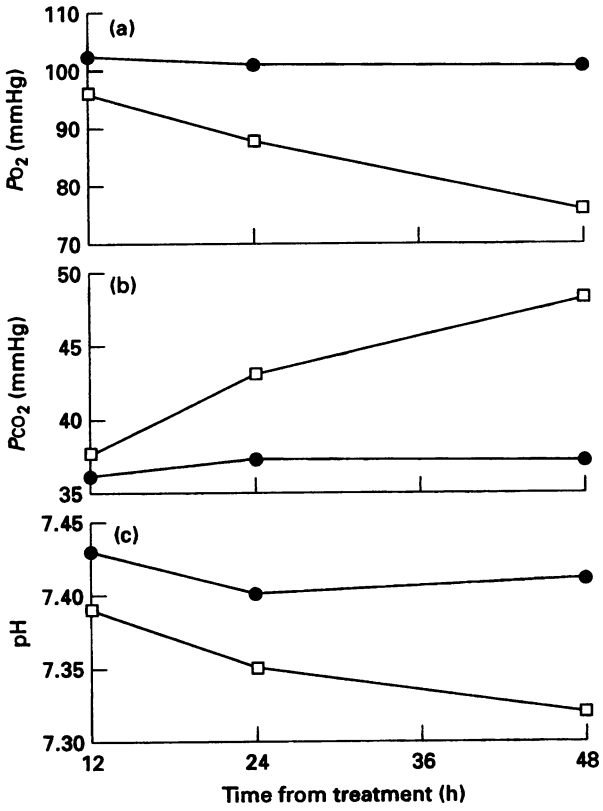

Figure 1. Time course of blood gas analysis values for control and endotoxin treated rats. ●, Untreated + saline instilled rats; □, endotoxin instilled rats. Error bars are not indicated because they would have been too close to the means, since standard error was a, less than 5% of the mean for Po_2; b, less than 3% of the mean for Pco_2; and c, less than 0.2% of the mean for pH, at all time points and in all experimental conditions. Differences between pairs of values were significant ($P < 0.005$) for the three parameters 24 and 48 hours after treatment.

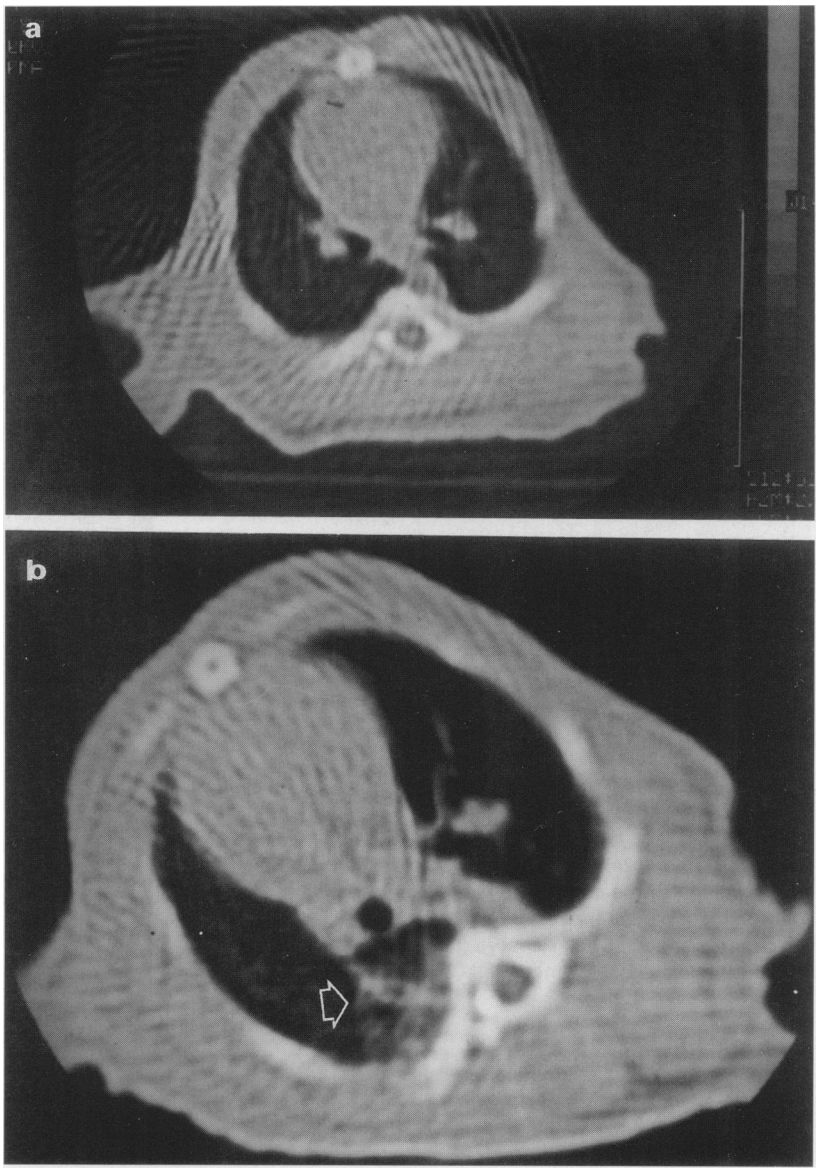

Figure 2. CT scan of a, an untreated rat lung and b, rat lung 48 hours after endotoxin instillation. A conspicuous parenchymal infiltrate is present in the subcarinal space of the treated rat (b, arrow), whereas the lung parenchyma appears normally aerated in control conditions.

microscopy, one-half of each lung of 25 rats (4 untreated, 6 at 48 hours after instillation of saline and 15 at all three time points after instillation of LPS) was fixed in Bouin's solution and embedded in paraffin. Sections were cut parallel to the frontal plane of the lung and stained with haematoxylin and eosin.

The lungs of 4 untreated rats, 6 rats 48 hours after saline treatment and 9 rats 48 hours after endotoxin treatment were used for morphometry. In one lung section per rat, cut along the longitudinal axis of the organ, the volume ratio of tissue to organ $\left(\frac{V_T}{V_O}\right)$ was evaluated by point counting with a square test lattice, with distance of test points (d) of 2 cm, at magnification $\times 500$. A total area of 0.9–1.1 mm^2 was analysed for each

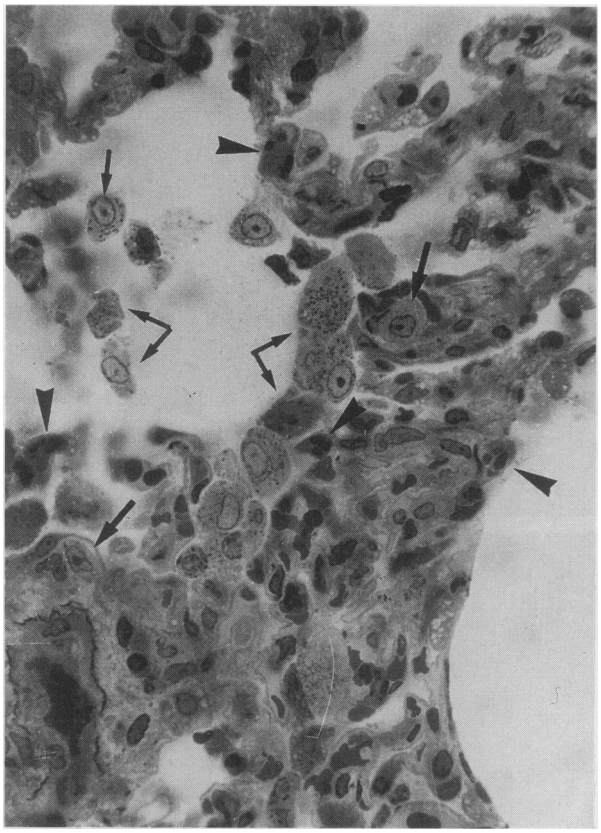

Figure 3. Rat lung 24 hours after endotoxin instillation. Some neutrophils (arrowheads) can be seen in the alveolar septa. Many immature macrophages are visible both in the septa (large arrows) and alveolar spaces (thin arrows). Semithin section stained with toluidine blue. ×650.

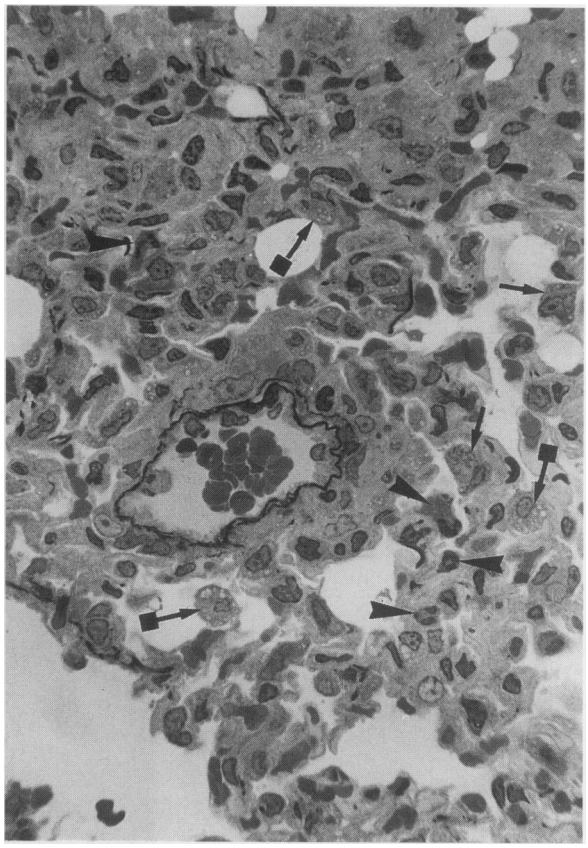

Figure 4. Rat lung 48 hours after endotoxin instillation. Neutrophils (arrowheads) and immature (arrows) and mature macrophages (arrows with squares) are shown. The exact localization of each cell type is shown only by electron microscopy. Capillaries are open even in heavily infiltrated areas. Semithin section stained with toluidine blue. ×450.

section. The ratio $\left(\frac{V_T}{V_O}\right)$ was computed by the number of test points on the tissue, including infiltrate when present (P_T), and those on the whole organ (tissue plus air spaces, P_O) from the equation $\left(\frac{V_T}{V_O}\right) = \left(\frac{P_T}{P_O}\right)$ (Weibel 1979).

One-half of each lung of 21 rats (2 untreated, 6 at 48 hours after saline instillation, 3 at 12 hours after endotoxin instillation, 3 at 24 hours after endotoxin instillation and 7 at 48 hours after endotoxin instillation) was prepared for electron microscopy. The tissue was divided into an apical, a middle and a basal third and then minced into small blocks. Some randomly selected blocks from each third of each lung were fixed in Karnovsky's solution in 0.1 mol/l cacodylate buffer, pH 7.4, post-fixed in 1% osmium tetroxide in 0.1 mol/l phosphate buffer, pH 7.4, and embedded in Epon 812. Semithin sections were used to identify the tissue blocks where an infiltrate was present.

Ultrathin sections from these blocks were stained with uranyl acetate, followed by bismuth subnitrate or lead citrate, and examined in an Elmiskop 102 (Siemens, Munich, Germany) electron microscope at 80 kV.

Figure 5. Rat lung 12 hours after endotoxin instillation. A neutrophil is shown within a capillary. Electron microscopy. ×13 000.

Statistical analysis

Means and standard errors are given in the results. The results were evaluated by Student's *t*-test applied one-tailed, since we did not consider the hypothesis that treated rats could improve above controls.

Probability levels of $P < 0.05$ were recorded and accepted as significant.

Results

Saline instilled rats were similar to controls in all respects, that is arterial gas analyses, CT and histology. Therefore, the data from untreated and saline-instilled rats were pooled together into a single control group for all comparisons.

Endotoxin instilled rats showed progressive hypoxaemia, hypercapnia and acidosis from 24 hours after treatment (Figure 1).

Diffuse, inhomogeneous, bilateral infiltrates were a common finding by CT in the lungs of rats 24 hours after endotoxin instillation and these were larger at 48 hours (Figure 2).

By light microscopy, focal infiltrates of neutrophils and mononuclear cells were evident 24 hours after endotoxin instillation (Figure 3) and became significantly more extensive with time (Figure 4). The volume ratio of tissue (including infiltrate) to organ was 0.5329 (standard error ±0.0343, range 0.3515–0.6563) in the controls and 0.6420 (standard error ±0.0366, range 0.4393–0.8132; $P < 0.05$ *vs* controls) in endotoxin treated rats. Forty-eight hours after treatment, eosinophilic, amorphous material was also found in some alveoli.

By electron microscopy, the evolution of infiltrates appeared as follows.

Twelve hours after endotoxin instillation, interalveolar septa contained many neutrophils and some monocytes; neutrophils were found only inside blood capillaries (Figure 5), whereas monocytes were found within both blood capillaries and interstitial space.

Twenty-four hours after endotoxin instillation, the picture of interalveolar septa was substantially the same as at 12 hours, i.e. blood capillaries contained many neutrophils and some monocytes as well. At this time point, several macrophages were found within alveoli. These cells were large and had a wide Golgi apparatus and a few, short projections on their surface. Characteristically they contained many homogeneously electron dense, round or cup-shaped primary lysosomes (Figure 6).

Forty-eight hours after endotoxin instillation, neutrophils were found only in the interstitial septa and within the alveoli, where they were much more numerous (Figure 7). Some monocytes were found within alveoli, which also contained many macrophages. These last cells were large and had an inconspicuous Golgi apparatus and many projections on their surface; these projections were sometimes thin and long, sometimes short and thick. Characteristically, they contained many round lysosomes which were homogeneously electron dense or with a dense core of varying size, sometimes wider than 1 μm (Figure 8).

The eosinophilic material turned out to be fibrin (Figure 8) in some alveoli and amorphous in others.

The alveolar lining was continuous and comprised many type II pneumocytes with lamellar bodies (Figure

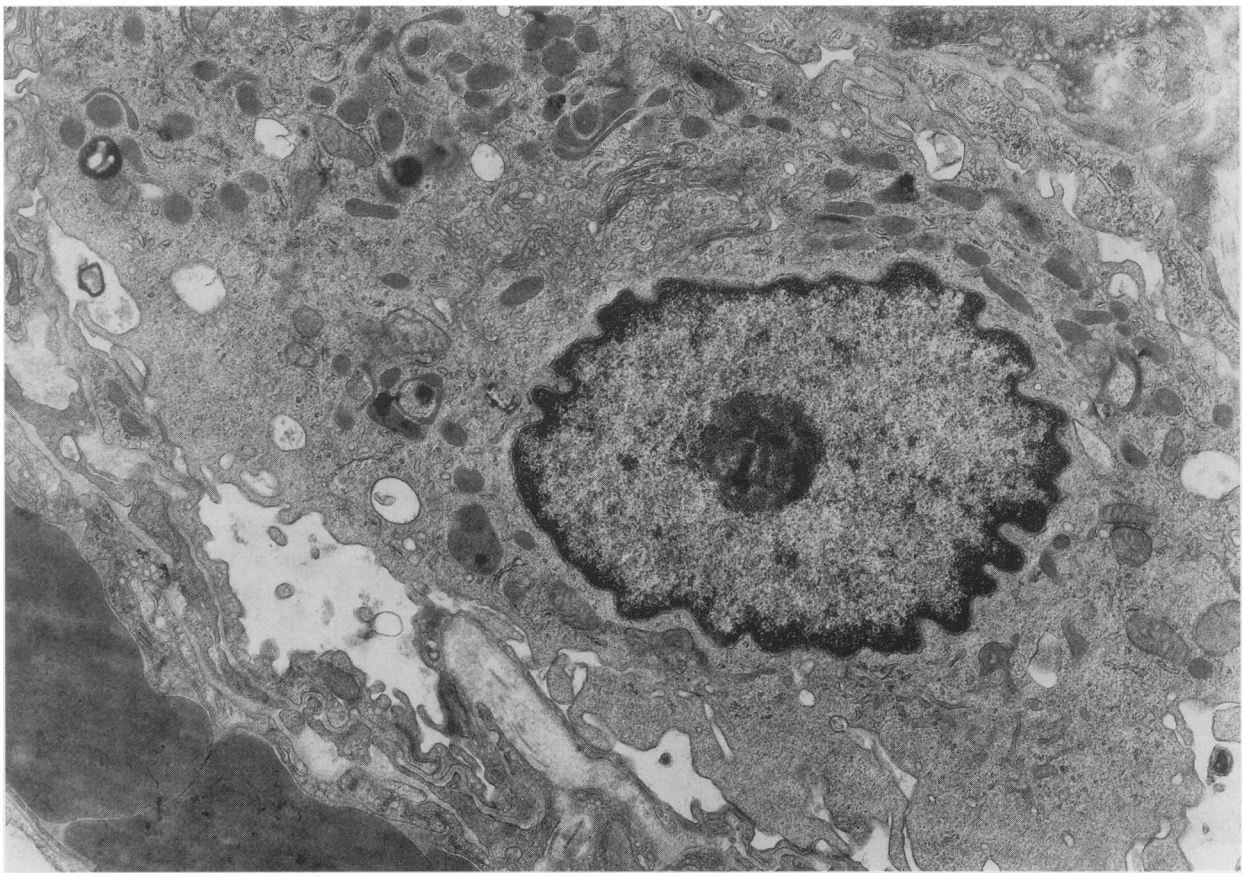

Figure 6. Rat lung 24 hours after endotoxin instillation. An immature macrophage with wide Golgi apparatus, many round and cup-shaped primary lysosomes and few short cell surface projections is shown inside an alveolus. Electron microscopy. ×11 000.

7). Some of these cells contained many free ribosomes and little rough endoplasmic reticulum, thus resembling immature cells (Figure 9).

Type I pneumocytes appeared as in controls. Interstitial fibroblasts were increased in number and size and richer in rough endoplasmic reticulum than when observed at previous time points (Figure 7).

Endothelial cells and subepithelial and subendothelial basement membranes were as in controls and capillaries remained open even in heavily infiltrated areas.

Discussion

In this research we followed the evolution of endotoxin induced experimental lung injury by blood gas analysis, CT, and light and electron microscopy. We have shown that intratracheal instillation of endotoxin causes in rats an acute respiratory failure within 48 hours accompanied by infiltration of mononuclear cells and neutrophils in the lungs.

Saline solution failed to reproduce the radiological, haematological and histological picture which followed endotoxin instillation; therefore, the observed pulmonary damage should be interpreted as caused by LPS.

Electron microscopy, in particular, let us identify and visualize in detail the cell types involved in the evolution of these infiltrates. This type of information had escaped a previous investigation in the rat, where continuous venous infusion of endotoxin had led to the appearance

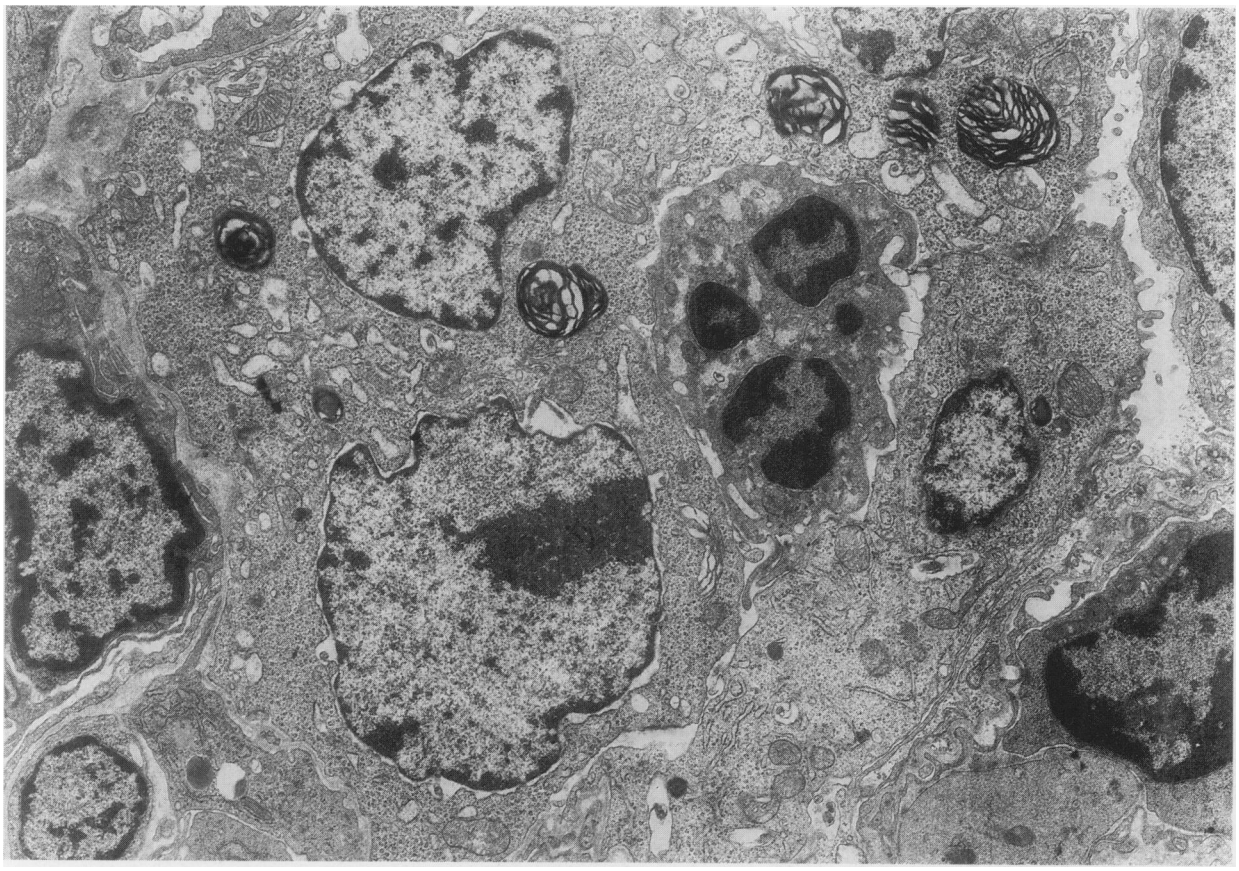

Figure 7. Rat lung 48 hours after endotoxin instillation. Four type II pneumocytes (two of them contain lamellar bodies) and an intra-alveolar neutrophil are shown. Electron microscopy. ×6500.

of neutrophils inside blood capillaries, interstitium and alveoli at the same time; in the alveoli, neutrophils were reported to colocalize with macrophages (Simons *et al.* 1991). In the present study, monocytes were found within both blood capillaries and interstitial spaces by 12 hours after treatment, whereas numerous macrophages were found within alveoli by 24 hours after treatment.

Macrophages were never found within the alveolar septa, only inside the alveoli; moreover, the structure of these cells was different at 24 from that at 48 hours after treatment, with pictures that can be interpreted as indicative of recruitment of monocytes from blood to alveoli soon after treatment, followed by differentiation of monocytes into macrophages and further maturation of these cells within alveoli. Neutrophils, however, although relatively frequent from early time points (12 hours) after treatment, remained restricted within blood capillaries until 24 hours and appeared to infiltrate interstitial spaces and, most importantly, the alveolar spaces only 48 hours after treatment.

Taken all together, these findings suggest that neutrophils contribute to early phases of endotoxin induced lung injury from within blood vessels and possibly at a later stage worsen the final picture by contributing to alveolar infiltrates. These findings further indicate that the neutrophil infiltrates form following the recruitment of monocytes and their differentiation into macrophages. Pre-existing lung macrophages did not seem to play a major role in this experimental model of lung injury. Endotoxin can cause leucocyte adhesion to endothelial cells and activation of these cells to secrete several biologically active mediators (Neuhof 1991). The

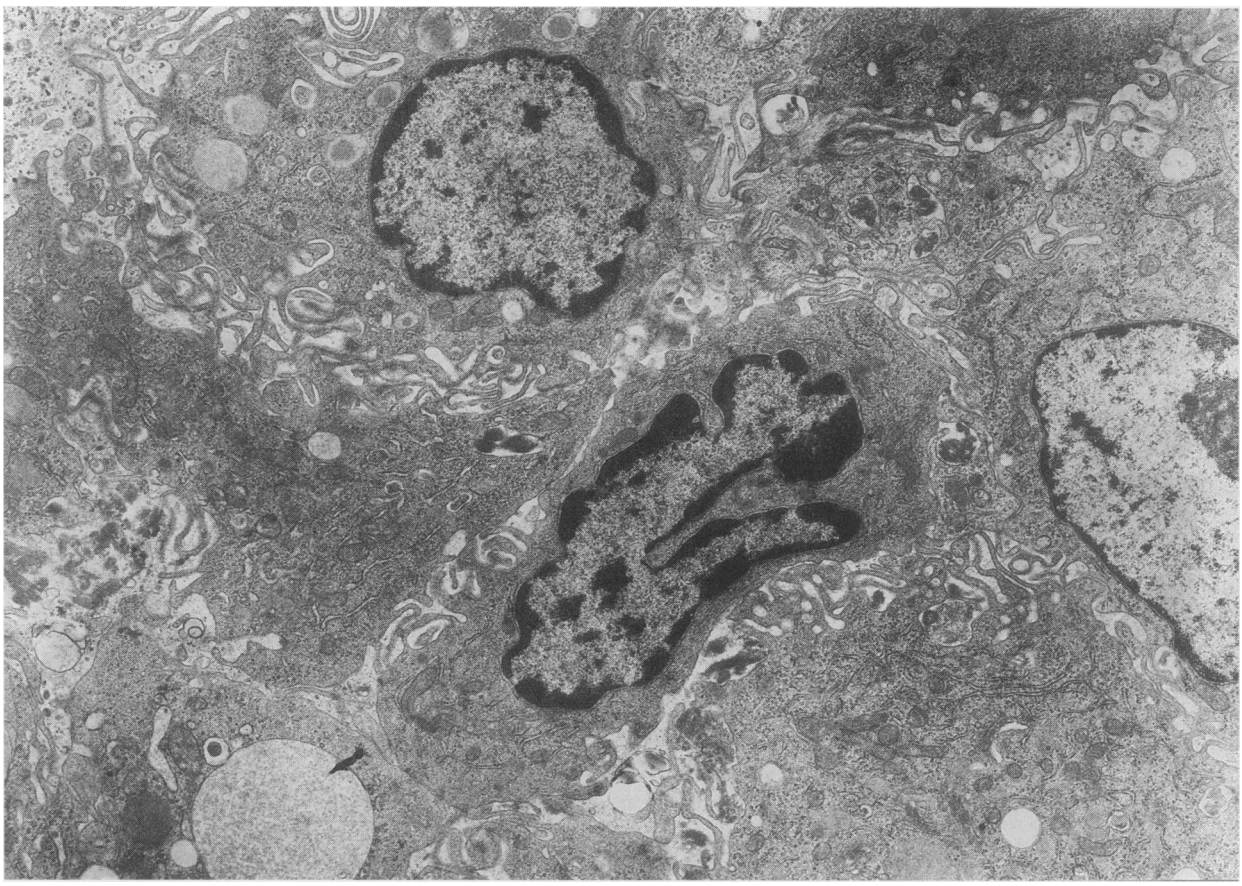

Figure 8. Rat lung 48 hours after endotoxin instillation. Intra-alveolar infiltrate includes macrophages and fibrin. Macrophages have many round lysosomes and thin and long cell surface projections. Electron microscopy. ×6500.

main types of leucocytes (neutrophils, monocytes and macrophages) we found involved in the lung infiltrates can also interact with each other due to the action of many of these mediators (Romagnani & Caligaris Cappio 1991).

This interpretation of the pathogenesis of endotoxin induced lung damage might also apply, at least in part, to human acute ARDS (for review see Hasleton 1983). Were this the case, there would be an initial phase when disease evolution might be blocked, before neutrophils have extravasated and monocytes have differentiated into infiltrated macrophages.

Relevant modifications of type II pneumocytes and interstitial fibroblasts were found at 48 hours after treatment. Type II pneumocytes were especially frequent at this time point and often had features of immature cells. This finding is in agreement with previous data (Simons *et al.* 1991) and suggests hyperplasia of these cells as part of a response to alveolar injury, as shown previously in other experimental models (Yuen & Sherwin 1971; Meyrick & Brigham 1983, Simons *et al.* 1991). At the same time point, interstitial fibroblasts became more frequent, larger, and richer in endoplasmic reticulum than in control conditions or at previous experimental time points. Leucocyte-derived mediators, including several cytokines, might be responsible for the activation of these cells (Neuhof 1991; Romagnani & Caligaris Cappio 1991) which, in

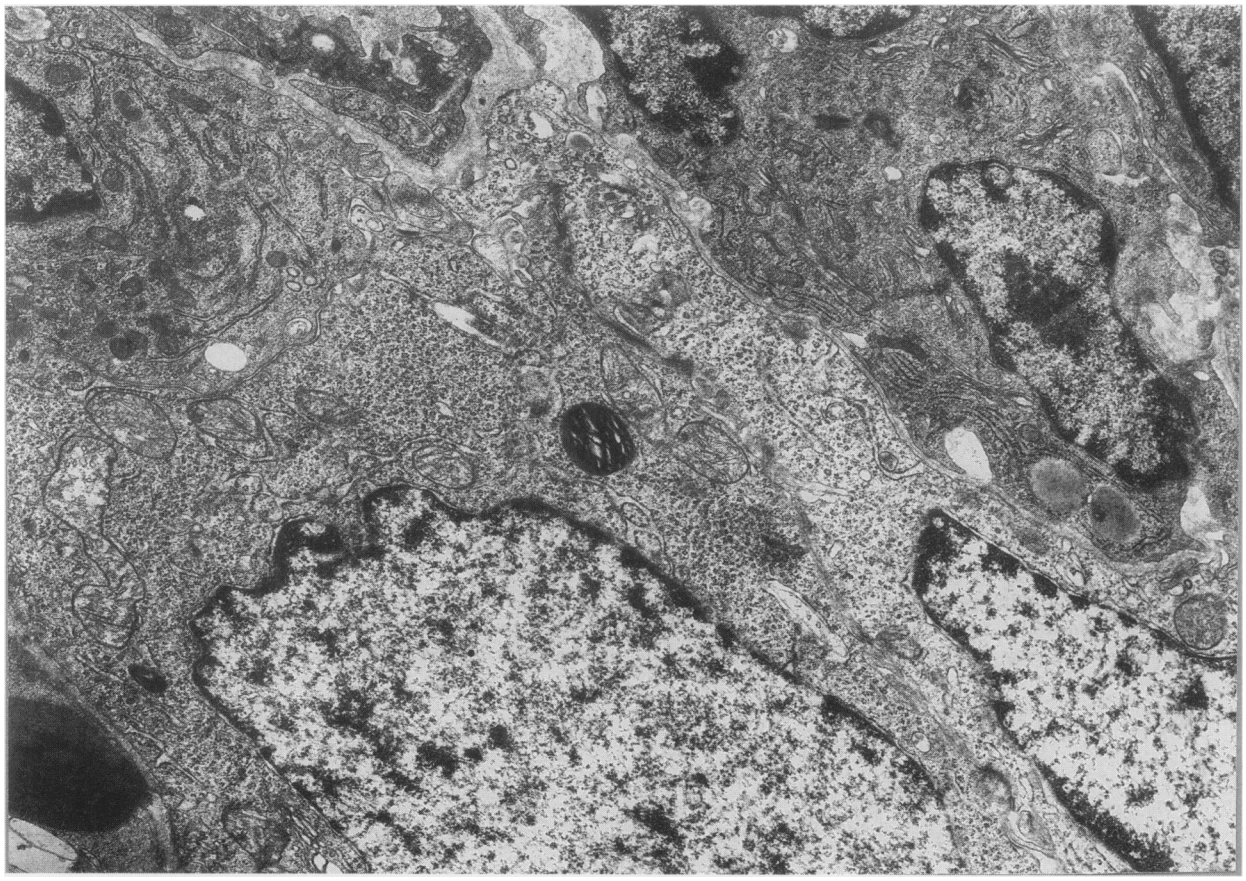

Figure 9. Rat lung 48 hours after endotoxin instillation since 48 hours. Two type II pneumocytes with many free ribosomes and little rough endoplasmic reticulum and an interstitial fibroblast (top right) with well developed rough endoplasmic reticulum and some lipid droplets are shown. Electron microscopy. ×13 000.

turn, might play a role in late development of fibrosis (Vaccaro & Brody 1978) as happens in humans surviving acute ARDS (Hasleton 1983; Murray *et al.* 1988).

Acknowledgements

The authors thank Dr F.M. Colonna for skilful technical assistance. This research was supported by the Italian Ministry of Universities, Science and Technology ('University funds – 40%' and 'University funds – 60%'), National Research Council (grant n.93.00402.04) and Regione Toscana (as part of the 3rd project of finalized health research).

References

Adembri C., Forzini R., Laviola S., Domenici Lombardo L., Romagnoli P., Consalvo M., De Gaudio R. & Novelli G.P. (1992) Un nuovo modello di insufficienze respiratoria acuta nel ratto. *Min. Anest.* **58,** 903–904.

Bachofen M. & Weibel E.R. (1982) Structural alterations of lung parenchyma in the adult respiratory distress syndrome. *Clin. Chest Med.* **3,** 35–56.

Esbenshade A.M., Newman J., Lams P., Jolles Y. & Brigham K. (1982)

Respiratory failure after endotoxin infusion in sheep: lung mechanics and lung fluid balance. *J. Appl. Physiol.* **53,** 967–976.

Fein A.M. Lippmann M., Holtzman M.H., Eliraz A. & Goldberg S.K. (1983) The risk factors, incidence and prognoses of ARDS following septicemia. *Chest* **1,** 20–42.

Glauser M.P., Zanetti G., Baumgartner J.D. & Cohen J. (1991) Septic shock: pathogenesis. *Lancet* **338,** 732–735.

Hasleton P.S. (1983) Adult respiratory distress syndrome – a review. *Histopathology* **7,** 307–332.

Kaplan R.L., Sahn S.A. & Petty T.L. (1979) Incidence and outcome of the respiratory distress syndrome in Gram-negative sepsis. *Arch. Intern. Med.* **139,** 867–869.

Meyrick B. & Brigham K.L. (1983) Acute effects of Escherichia Coli endotoxin on the pulmonary microcirculation of anesthetized sheep. Structure function relationships. *Lab. Invest.* **48,** 458–470.

Murray J.F., Matthay M.A., Luce J.M. & Flick M.R. (1988) Pulmonary perspectives: an expanded definition of the adult respiratory distress syndrome. *Am. Rev. Respir. Dis.* **138,** 720–723.

Neuhof H. (1991) Actions and interactions of mediator systems and mediators in the pathogenesis of ARDS and multiorgan failure. *Acta Anaestesiol. Scand.* **35 (Suppl. 95),** 7–14.

Ooi H., Arakawa M. & Ozawa H. (1994) A morphological study of acute respiratory tract lesions in a lipopolisaccharide instilled rat model. *Arch. Histol. Cytol.* **57,** 87–105.

Romagnani S. & Caligaris Cappio F. (1991) *Immunologia Clinica e Allergologia.* Torino, UTET.

Simons R.K., Maier R.V.V & Chi E.Y. (1991) Pulmonary effects of continuous endotoxin infusion in the rat. *Circ. Shock* **43,** 233–243.

Tate R.M. & Repine J.E. (1983) Neutrophils and the adult respiratory distress syndrome. *Am. Rev. Resp. Dis.* **128,** S52–59.

Vaccaro C. & Brody J. (1978) Ultrastructure of developing alveoli. The role of interstitial fibroblasts. *Anat. Rec.* **192,** 467–480.

Weibel E.R. (1979) *Stereological Methods.* Volume 1. London, Academic.

Wheeldon E.B., Walker M.E., Murphy D.J. & Turner C.R. (1992) Intratracheal aerosolization of endotoxin in the rat. A model of the adult respiratory distress syndrome. *Lab. Anim.* **26,** 29–37.

Wiener-Kronish J.P., Gropper M.A. & Matthay M.A. (1990) The adult respiratory distress syndrome: definition and prognosis, pathogenesis and treatment. *Br. J. Anaesthesiol.* **65,** 107–129.

Yuen T.G.H. & Sherwin R.T. (1971) Hyperplasia of type II pneumocytes and nitrogen dioxyde (10 ppm) exposure. *Arch. Environ. Health* **22,** 178–206.